Extended Abstracts of the 2016 International Conference on Solid State Devices and Materials, Tsukuba, 2016, pp185-186

D-1-04(Invited)

# Valley Hall Effect in Bilayer Graphene with Electrically Broken Inversion Symmetry

Yuya Shimazaki[1], Michihisa Yamamoto[1, 2], Ivan V. Borzenets[1], Kenji Watanabe[3], Takashi Taniguchi[3] and Seigo Tarucha[1, 4]

[1] Department of Applied Physics, Univ. of Tokyo
7-3-1 Hongo, Bunkyo-ku, Tokyo 113-8656, Japan
Phone: +81-3-5841-6842 E-mail: shimazaki@meso.t.u-tokyo.ac.jp
[2] PRESTO JST
4-1-8 Hon-cho, Kawaguchi-shi, Saitama 331-0012, Japan
[3] National Institute for Materials Science
1-1 Namiki, Tsukuba-shi, Ibaraki, Japan, 305-0044
[4] Center for Emergent Matter Science (CEMS), RIKEN
2-1 Hirosawa, Wako, Saitama, Japan, 361-0198

**Abstract**

**"Valleytronics" is a newly developed concept for electronics utilizing the occupation degree of freedom of valleys as an information carrier. Spatial inversion symmetry broken honeycomb lattice systems are ideal materials for valleytronics. Due to valley contrasting Berry curvature, these systems show valley Hall effect and its inverse effect, which enable generation and detection of a pure valley current. Here we used dual-gated bilayer graphene to break the spatial inversion symmetry electrically. At 70K, around charge neutrality point, we found that large nonlocal resistance emerges under displacement field and it scales cubically with the local resistivity by tuning the displacement field. This is an evidence of the pure valley current mediating the nonlocal transport and the valley Hall effect in spatial inversion symmetry broken bilayer graphene.**

## 1. Introduction

Charge and spin of electrons are well-defined quantum numbers. Spintronics is a technique which utilizes the spin degree of freedom as an information carrier in solid state devices. The discovery of spin Hall effect and its inverse effect, which enable electrical generation and detection of spin current, widened the range of application of the spintronics. Certain specific crystal structures result in degenerate local minima or maxima called "valleys" in the band structure (Fig. 1 (a)). The occupation degree of freedom of valleys is well-defined quantum number, and a newly developed concept for utilizing this valley degree of freedom as an information carrier is called "valleytronics". Honeycomb lattice systems such as graphene and transitional metal dichalcogenides are ideal platform for the valleytronics. When inversion symmetry of these systems are broken, effective magnetic field called Berry curvature emerges. Because the sign of this Berry curvature is dependent on valleys, these systems show valley dependent Hall effect known as valley Hall effect [1] (Fig. 1 (b)). The valley Hall effect and its inverse effect enable electrical generation and detection of a pure valley current, which is interpreted as an analogy of pure spin current and does not accompany net charge flow.

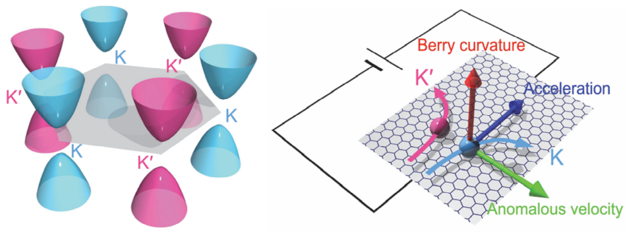


Fig. 1 (a) Band structure of gapped bilayer graphene. K and K' represent valley index. (b) Schematic image of the valley Hall effect.

Valley Hall effect was demonstrated in structurally inversion symmetry broken systems such as $MoS_2$ [2] and monolayer graphene/h-BN superlattice [3]. For the case of bilayer graphene (BLG), however, a perpendicular electric displacement field (*D*) can be used to break inversion symmetry. The tunable *D* allows for further controllability of the valley Hall effect and unambiguous detection of the pure valley current.

## 2. General Instructions

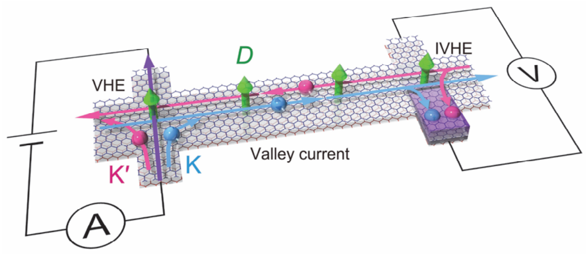


Fig. 2 Schematic image of the valley current mediated nonlocal transport and the setup of the nonlocal resistance measurement.

To investigate the valley Hall effect (VHE), we utilized nonlocal resistance measurement. In Fig. 2, charge current is injected at the left side across the Hall bar. VHE at the left side generates valley current along the Hall bar, and it is detected as voltage signal by inverse valley Hall effect (IVHE) at the right side. Nonlocal resistance ($R_{NL}$) is defined by the detected voltage divided by the injected current. Using an analogy of the nonlocal resistance by spin Hall effect and inverse spin Hall effect [4], $R_{NL}$ is expected to follow the following equation:

$$R_{NL} = \frac{W}{2l_v}\left(\sigma_{xy}^{VH}\right)^2 \rho^3 \exp\left(-\frac{L}{l_v}\right). \qquad (1)$$

$W$ and $L$ are the channel width of the Hall bar and the lateral distance between the current injection probe and the voltage detection probe, respectively. $l_v$ is inter-valley scattering length. $\sigma_{xy}^{VH}$ and $\rho$ are the valley Hall conductivity and local resistivity, respectively. $\rho$ has maximum value at the charge neutrality point (CNP) and also increases with increasing the magnitude of $D$ due to the enhancement of the band gap [5]. For the case of the intrinsic origin of the valley Hall effect described above, $\sigma_{xy}^{VH}$ has maximum value at the CNP. If the band gap size is larger than the temperature energy scale, $\sigma_{xy}^{VH}$ has constant value. These dependencies lead to maximum $R_{NL}$ at the CNP for the carrier density dependence and increasing $R_{NL}$ as increasing the magnitude of $D$. Furthermore, for the constant $\sigma_{xy}^{VH}$ regime, the nonlinear, cubic scaling relation $R_{NL} \propto \rho^3$ is expected from eq. (1).

We utilized dual-gated structure to control the perpendicular electric displacement field $D$, and carrier density independently [5]. To keep the quality of the device, we encapsulated BLG between h-BN insulating layers. Both BLG and h-BN are obtained by mechanical exfoliation technique and they are stacked using a dry transfer technique. BLG is shaped into a Hall bar whose $W$ and $L$ are 1um and 3.5um, respectively.

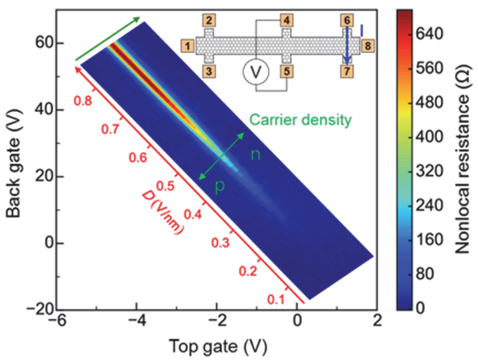


Fig. 3 Electric displacement field ($D$) and carrier density dependence of the nonlocal resistance. $D$ is tuned along the red arrow. Carrier density is tuned along the both ended green arrow. Inset: The configuration of nonlocal resistance measurement.

Fig. 3 shows the measurement result of $R_{NL}$ against top and back gate voltages at 70K. As $D$ increases, $R_{NL}$ peak appears around CNP and increases as expected. At the highest $D$, the size of the signal is 3 order of magnitude larger than the trivial current diffusion contribution calculated from the van der Pauw formula.

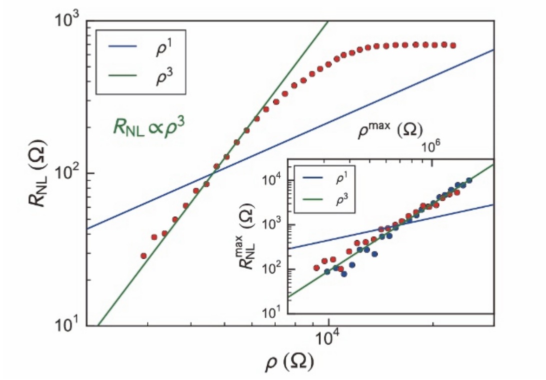


Fig. 4 Scaling relation between $\rho$ and $R_{NL}$ at the CNP by tuning $D$. Inset : Scaling relation obtained from other device. Red points and blue points are obtained from $D > 0$ and $D < 0$, respectively.

Fig. 4 shows the relation between $\rho$ and $R_{NL}$ at the CNP by tuning $D$. We observe the cubic scaling $R_{NL} \propto \rho^3$ for $\rho <$ 7kΩ. The cubic scaling is reproduced in other device for the both polarity of $D$ (Fig. 4 inset). We also observed the cubic scaling from temperature dependence at the CNP. On the other hand, the deviation from the cubic scaling appeared for $\rho >$ 7kΩ (Fig. 4). One possible reason for this deviation is the change of the valley Hall conductivity in the hopping conduction regime. In the temperature dependence, both $\rho$ and $R_{NL}$ showed the activation behavior. By comparing the activation energy of $\rho$ and $R_{NL}$ in the band conduction regime ($E_L$ and $E_{NL}$, respectively), we find $dE_{NL}/dD \sim 3dE_L/dD$. This factor three is also expected from the cubic scaling.

## 3. Conclusions

We detected the huge nonlocal resistance signal around the CNP by applying perpendicular displacement electric field $D$ in the dual-gated bilayer graphene device. We find the cubic scaling relation $R_{NL} \propto \rho^3$ from both $D$ and temperature dependence at the CNP. As evidenced by these observations, we detected the valley current mediated nonlocal transport due to the valley Hall effect and the inverse valley Hall effect [6, 7]. Similar results in bilayer graphene are also reported by another group around the same time [8].

## Acknowledgements

We acknowledge fruitful discussion with L. S. Levitov, J. C. W. Song, M. Koshino, M. Ezawa and N. Nagaosa.

## References

[1] D. Xiao *et al.*, Phys. Rev. Lett. **99** (2007) 236809.
[2] K. F. Mak *et al.*, Science **344** (2014) 1489.
[3] R. V. Gorbachev *et al.*, Science **346** (2014) 448.
[4] D. A. Abanin *et al.*, Phys. Rev. B **79** (2009) 035304.
[5] J. Oostinga *et al.*, Nature Materials **7** (2007) 151.
[6] Y. Shimazaki *et al.*, Nature Physics **11** (2015) 1032.
[7] M. Yamamoto *et al.*, J. Phys. Soc. Jpn. **84** (2015) 121006.
[8] M. Sui *et al.*, Nature Physics **11** (2015) 1027.